Limnol. Oceanogr., 37(8), 1992, 1738–1753

Early diagenesis in a marine sapropel, Mangrove Lake, Bermuda

Bernard P. Boudreau
Department of Oceanography, Dalhousie University, Halifax, Nova Scotia B3H 4J1

Donald E. Canfield
School of Earth and Atmospheric Sciences, Georgia Institute of Technology, Atlanta, 30332-0340

Alfonso Mucci
Department of Geological Sciences, McGill University, Montréal, Quebec H3A 2A7

Abstract

The pore waters of a marine sapropel in Mangrove Lake (Bermuda) have been analyzed for a suite of diagenetically sensitive species, i.e. pH, SO_4^{2-}, ΣH_2S, Ca^{2+}, ΣCO_2, ΣNH_4, ΣPO_4, Fe^{2+}, and Mn^{2+}. We have also measured a ^{210}Pb depth profile (suggesting a burial velocity of 0.94 cm yr^{-1}) and experimentally determined the rate constant for sulfate reduction (0.062 yr^{-1}).

Waves and turbulence have mixed sediment and pore waters to a depth of 15 cm. However, both stoichiometric and transport-reaction models argue that molecular diffusion dominates solute transport beneath this mixed zone and that the pore waters are open to diffusion despite rapid burial. Diagenetic modeling shows further that diffusion accounts for 95% of the SO_4^{2-}, ΣH_2S, and ΣCO_2 fluxes below the mixed layer. Comparison of model results with sulfur burial fluxes indicates that at least 94% of the generated ΣH_2S diffuses out of the sediments. The pore-water ΣCO_2 is also within 5% of that predicted by our models. The C:N ratio of the decaying organic matter is calculated to be between 3.86 and 6.87, which is less than half that obtained by analysis of the solids.

The carbonate chemistry of the pore waters suggests that they are nearly saturated with respect to aragonite in the mixed zone, even though this mineral has not been identified in the solids. Precipitation in the mixed zone is confirmed by comparing the observed dissolved Ca profile with that expected for conservative behavior.

Oxidation of organic matter is recognized as the most important diagenetic reaction in marine sediments, and its effects have been studied extensively (e.g. Aller 1980; Emerson et al. 1980; Froelich et al. 1979; Jahnke et al. 1982). However, the mixture of silicates, carbonates, and organic solids that is typical of most sediments leads to complex pore-water chemistries as a result of a large number of often poorly understood interactions (e.g. Boudreau and Canfield 1988; Canfield and Raiswell 1991). Sediments composed of a single solid phase diminish the number of reactions that must be considered and, therefore, simplify the diagenetic interpretation of observed pore-water profiles. Consequently, a nearly pure organic matter sediment, called a sapropel, deserves intensive examination.

Just such a sapropel is accumulating in saline Mangrove Lake on Bermuda (Hatcher 1974), and various aspects of its chemistry have been reported (Hatcher 1978; Hatcher et al. 1982; Spiker and Hatcher 1984; Orem et al. 1986). Unfortunately, the nature and spatial resolution of these data are insufficient to obtain a quantitative appreciation for the early diagenesis of this sediment, i.e. what happens in detail in the first 50 cm where organic matter oxidation is most vigorous. Two groups of scientists are currently studying this lake with the aim of resolving this situation. Our results are reported here, those of the other group are reported by Mackenzie et al. (in press).

Acknowledgments

We are grateful to John N. Smith for the ^{210}Pb determinations. Barry Hargrave contributed to the success of our field trip. Fred Mackenzie encouraged our efforts and supplied valuable information about the sampling site. Q. Siddiqui provided identification of the ostracods. The Bermuda Biological Station (BBS) acted as our host and supplied needed equipment. We thank R.A. Berner, R. Marinelli, R. Stauffer, and two anonymous persons for reviews of the manuscript.

The work was supported by the Natural Sciences and Engineering Research Council of Canada (operating grants to B.P.B. and to A.M.). Don Canfield was funded by an NRC (USA) postdoctoral fellowship.

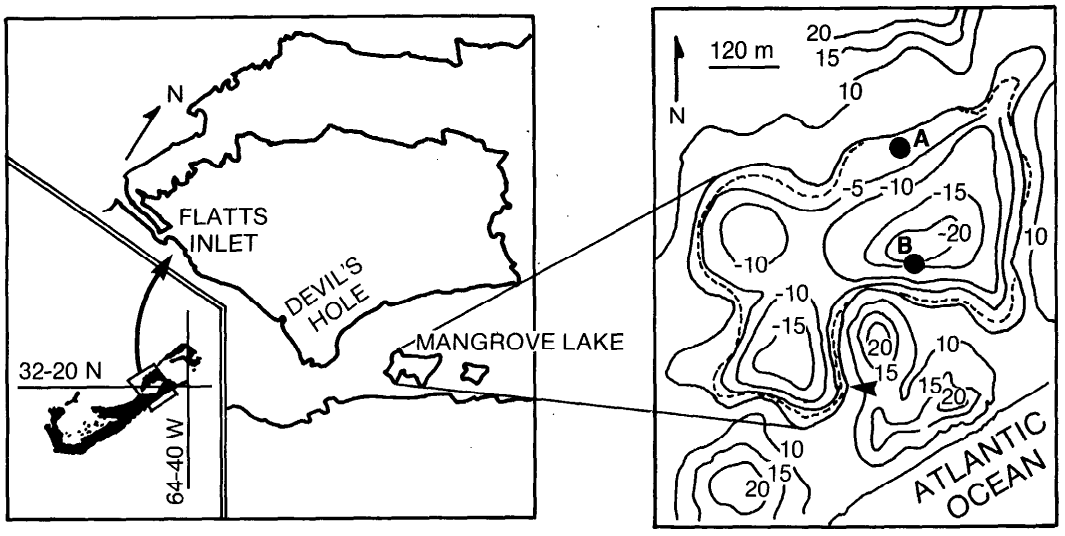

Fig. 1. Map showing Mangrove Lake. The sampling location is marked A on the contour map. Also shown is the Hatcher et al. (1982) sampling site (B). The contours represent height of the bedrock surface in meters above the mean sea level. The lake is filled with sediment to within 50–100 cm of the surface. Dashed line indicates the farthest extent of mangrove growth into the lake.

Our study was initiated as part of a larger long-term project to understand the controls on pore-water pH in marine sediments. The pH of pore waters may be influenced by silicate reactions that are difficult to characterize (e.g. Mackin and Aller 1989); therefore, a sapropel that is poor in silicate minerals presents an attractive environment to study. Although it is still our aim to use the data in this paper to this end, the present contribution contains our initial investigation of the pore-water chemistry of Mangrove Lake and our interpretation of these results separate from the issue of pH control.

Background and methods

Setting—Figure 1 displays the location of the lake. It is ~300 × 400 m in size and occupies an interdune depression. Details of the geological setting and circumstances that led to its formation are given by Hatcher et al. (1982).

The lake waters are of normal seawater salinity (30–35). Thomas et al. (1991) have conducted a hydrological survey and established that seawater is supplied by fissures on the south side of the lake (arrow in Fig. 1) that are somehow connected to the ocean on the south side of the island. Thomas et al. showed further that the tidal range is only 1.4 cm, which indicates a highly dampened input system. During our visit, we observed no tidal variation outside of this range. There is no appreciable source of fresh surface water to the lake; there may be some groundwater input (Orem et al. 1986), but it must be small considering the high stable salinity of the lake water. Our sampling site is shown in Fig. 1 along with that reported by Hatcher et al. (1982). The water depth at our site was <1 m.

Sediment—The sediment cored in our study was an organic ooze (sapropel), primarily composed of phytoplankton (algae) remains with minimal amounts of mangrove debris (Hatcher et al. 1982; Orem et al. 1986). A detailed description of the organic geochemistry of this sediment can be found elsewhere (Hatcher 1978; Hatcher et al. 1982; Spiker and Hatcher 1984).

Coring and pore-water sampling—Coring was accomplished by having a swimmer insert a 1-m Plexiglas tube (5.5-cm i.d.) into the sediment, and capping the top, then the bottom, as the core emerged from the sediment. Although the sediment material was highly flocculant, we are reasonably confi-

dent that our coring technique did not disturb it appreciably. The sediment–water interface was distinctly apparent in the core and there was little suspended material in the trapped overlying water.

The core tube was predrilled at 2.5-cm intervals with holes equal to the outer diameter of the tip of a 60-ml syringe. These holes were covered with strips of plastic electrical tape surrounding the core. Subsampling of the core proceeded immediately and was performed by puncturing the tape with a blade and inserting the syringe tip; the tape acted as a gasket, limiting air entry into the syringe. Starting from the top port down, all the sediment (solids plus liquid) in a sampling interval was drawn into the syringe without exposure to air.

The samples were then taken to the BBS (Bermuda Biological Station) laboratory where the content of the syringes was transferred to squeezers (Reeburgh 1967) in a N_2-filled glove bag. This transfer was carried out within 1 h of the initial sampling. Pore waters were extracted under ~ 3 kg cm^{-2} of nitrogen pressure and filtered simultaneously through a glass-fiber filter and a 0.45-μm Millipore filter into a clean 60-ml syringe, all without atmospheric contact. We obtained 30–50 ml of pore water at each depth interval. (Oxidation of the samples was unlikely due to the short time between collection and processing, and the fact that all sample manipulations were performed in a N_2-filled glove bag.)

The filtered pore waters were returned to the glove bag and subdivided into a number of clean vials for specific analyses at BBS (i.e. pH, titration alkalinity, ΣH_2S, ΣNH_3, reactive-ΣPO_4), at McGill University (i.e. salinity, SO_4^{2-}, Ca^{2+}, Fe^{2+}, Mn^{2+}), and at NASA Ames (i.e. SO_4^{2-}). The solid residues on the filters were analyzed for ^{210}Pb at BIO and total S at McGill.

Analytical methods—Sediment porosity was determined on a core taken in close proximity to the working core. Porosity was calculated from the water loss after freeze-drying, assuming pore-water and dry organic sediment densities of 1.02 and 1.5 g cm^{-3}, respectively. Although the dry organic sediment density is unknown, the porosity is not affected significantly if this value is in the likely range of 1.0–2.0 g cm^{-3}.

The pH was measured in the laboratory on the squeezed and filtered pore waters with a combination glass electrode previously calibrated on the NBS (i.e. 6.862, 7.413, and 9.18 at 25°C; Bates 1973) and Hansson's (1973) Tris (i.e. 8.074 at $S = 35$ and 25°C) buffer scales. The electrode was fitted with a piece of Tygon and Parafilm to produce an air-tight seal when introduced into the neck of the sample vial leaving no headspace gas. Results are comparable to those obtained on-site by punching the electrode directly into sediment collected in a core adjacent to the working core. Measurements of pH were corrected for in situ temperature with the equation of Millero (1979). All pH measurements are reported on the Tris buffer scale, and we believe they are much better than ± 0.1 pH units. (Comparison to punch-in pH measurements in an adjacent core without temperature control indicates agreement to within ± 0.1 pH units, but this cannot be interpreted as true verification.)

Chlorinity and calcium concentrations were determined by potentiometric titrations with $AgNO_3$ and EGTA (Lebel and Poisson 1976) solutions, respectively. The titrant solutions were standardized with IAPSO standard seawater.

Dissolved sulfate was measured in alternating samples by two independent methods. The sulfate analyses conducted at McGill were obtained by a potentiometric back-titration of Ba^{2+} with EGTA following $BaSO_4$ precipitation and removal of interfering ions (Mucci 1991). The other set of sulfate measurements was made at NASA Ames. In this case, the pore water was passed through 0.45-μm Nuclepore filters. After appropriate dilutions, sulfate was measured on a Dionex model 2000 ion chromatograph. The sulfate values from these two methods produced a totally consistent depth profile (Fig. 2). In both cases, the pore-water samples were degassed and frozen for transport and, in the case of the samples destined for Ames, also acidified.

Total dissolved sulfide was measured colorimetrically (Cline 1969). All sample dilutions and color formations were per-

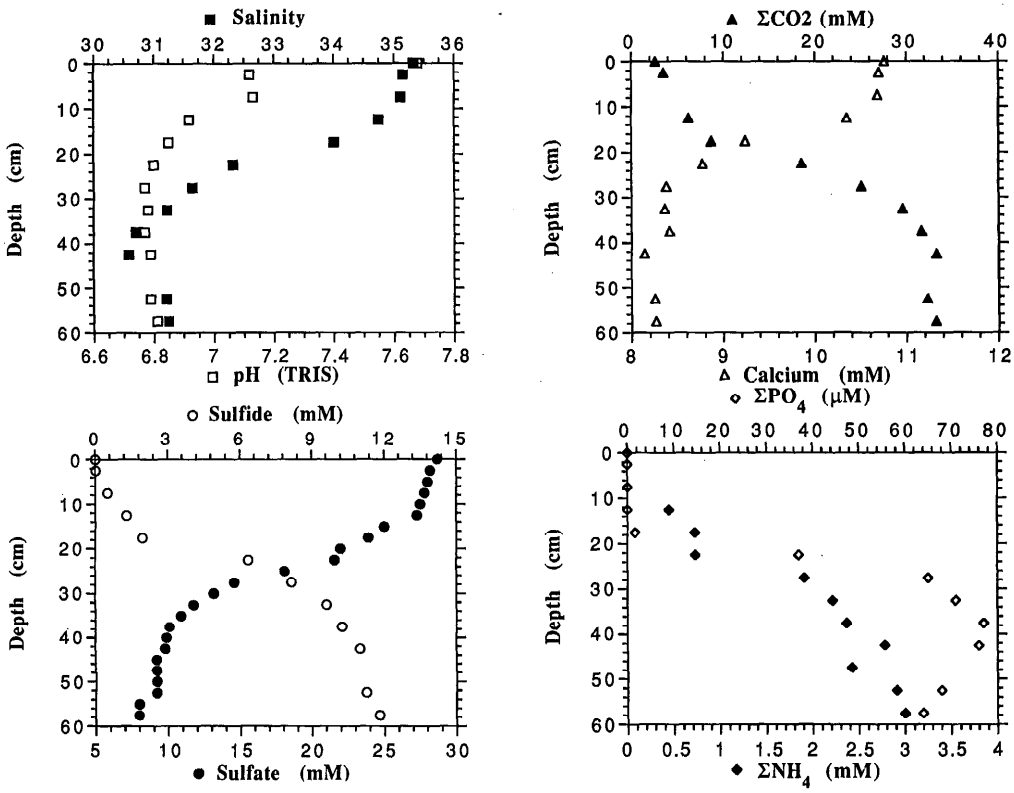

Fig. 2. Depth profiles of the major pore-water species in the sediments of Mangrove Lake. The surface pH value is nearly hidden underneath the surface salinity point (upper left). With regard to the sulfate profile, the second data point (at 2.5 cm) and every other sample thereafter was analyzed by the method of Mucci (1991). The intervening data were obtained by the more traditional method described in the text.

formed immediately after pore-water collection in a N_2-purged glove bag to avoid air oxidation of sulfide. Dissolved NH_3 and P were determined colorimetrically (Grasshoff 1976). Estimated precision on PO_4, NH_3, and sulfide is better than $\pm 10\%$ in each case. Dissolved Fe and Mn concentrations were obtained with flameless (graphite furnace) atomic adsorption spectrophotometry with external aqueous standards of similar salinity with a resulting precision of $\pm 10\%$.

Potentiometric Gran titrations (Gran 1952) with a dilute HCl solution were performed to obtain titration alkalinity values. This acid titrant was standardized with a Na_2CO_3 solution. The atmosphere above the titration vessel was constantly purged with a stream of nitrogen to inhibit oxidation of H_2S. The precision of this determination is better than 0.6%.

Total CO_2 was calculated from carbonate alkalinity, A_c, and pH. A_c was itself calculated from the total titration alkalinity, corrected for the contributions from HS^-, NH_4^+, $H_2PO_4^-$, HPO_4^{2-}, PO_4^{3-}, and dissociated boric acid. The dissociation constants used in these calculations are for the Tris buffer scale (i.e. Johansson and Wedborg 1979 for the phosphoric acid system, Millero et al. 1988 for the dissociation of H_2S, and Johansson and Wedborg 1980 for NH_3). Although the precision of the titration alkalinity is on the order of $\pm 0.6\%$, the cumulative error associated with the evaluation of A_c (i.e. pH, protolytic component concentrations, and dissociation constants) is more likely on the order of 5%. We re-

Table 1. Total S, Fe, and C (% dry wt), and the C:N ratio of the sediments in Mangrove Lake, August 1989, at location A (Fig. 1).

Depth (cm)	S	Fe	C	C:N (mol mol^{-1})
	(%)			
0–2.5	>0.66*		54†	16.5†
2.5–5	>0.46*		46†	12.4†
5–7.5	0.73			
5.5–10	0.86	0.34		
10–12.5	0.78		46	11.4
12.5–15	1.00		33	8.7
15–17.5	0.93		39	10.1
17.5–20	0.82		44	10.8
22.5–25	0.86	0.35	47	12.2
27.5–30	0.78		34	8.7
32.5–35	0.86		33	8.9
37.5–40	1.12	0.55	35	10.4
42.5–45	1.38		38	12.4

* Minimum values. Initial estimates were too low, and we had to readjust the titrant concentration. The first two sample depths could not be redone due to insufficient sample.

† Untreated sediment, includes both organic and inorganic C. All others are weak-acid treated and consequently are carbonate-free.

peated these calculations with NBS scale constants and found only small differences in calculated A_c and saturation states. Calculations of the thermodynamics of the carbonate system utilized the Tris buffer scale constants recommended by UNESCO (1987).

Rates of sulfate reduction were measured with $^{35}SO_4^{2-}$ (Jørgensen 1978). Sediment for rate measurements was collected immediately in duplicate from the core tube, as described above, into 5-ml plastic syringes with one end cut off. After collection, the open end of the 5-ml syringe was sealed with a butyl-rubber serum bottle-top. Within 1 h, 8 μCi of label was introduced with a Hamilton syringe through the rubber top. Sediment was incubated for 4 h in the dark within ± 2°C of ambient sediment temperature. Incubations were stopped by freezing. Radiolabeled sulfide was collected by distillation with an acidic chromous chloride solution (Canfield et al. 1986; Thode-Anderson and Jørgensen 1989), using a pyrite-rich coastal sediment as a sulfide carrier, and also adding ~1 g of sodium sulfate to reduce blanks. Rates were calculated as described by Jørgensen (1978).

As part of our study, we also determined the C, N, total S, and Fe content of the solids (Table 1). The C and N of the sediments were determined on most of the samples after treatment of the freeze-dried sediment with 1 N HCl to remove the carbonate fraction. These samples were subsequently centrifuged, decanted, and rinsed twice with deionized water, before being freeze-dried anew and homogenized. Analyses were performed on a Carlo-Erba elemental analyzer. The reproducibility of these measurements was poor, but typically on the order of 10%. As noted in Table 1, the first two samples were analyzed without acid treatment, and these results represent total C.

For S, variable weights of solid sediment were washed with distilled water and freeze-dried. These samples were then combusted in a LECO furnace and total S oxidized as SO_2. This resulting SO_2 was stripped of halogens and particulate matter and then bubbled in an acidic standardized iodine-iodide solution in the presence of a starch indicator. The consumed iodide was back-titrated with a standardized iodate solution, and the results were converted to %S on a dry weight basis (*see Table 1*). For total Fe, the samples were subject to sequential acid digestion of the total sediment with aqua regia, HF, and H_2SO_4 (Canfield 1989). Fe was then analyzed by atomic absorption spectroscopy.

Finally, ^{210}Pb was determined by α-particle counting of ^{210}Po. Details of this methodology are given by Smith and Walton (1980) and are not repeated here.

Results

Results of the pore-water analyses are displayed in Fig. 2. The salinity systematically drops from 35.3 at the sediment–water interface to ~31 at 50 cm—a change of ~17%. The elevated salinity of the surface waters can be attributed to a drought that persisted through 1989. Small salinity variations in this lake resulting from evaporation-precipitation have been noted by Hatcher et al. (1982) and Orem et al. (1986). Measurements of temperature (not shown) also indicate the presence of a temperature gradient, falling from 32°C in the surface waters to 28.5°C at a depth of 50 cm in the sediment. The sediment porosity is essentially constant at 0.955 ± 0.005.

The profiles for the dissolved species, ex-

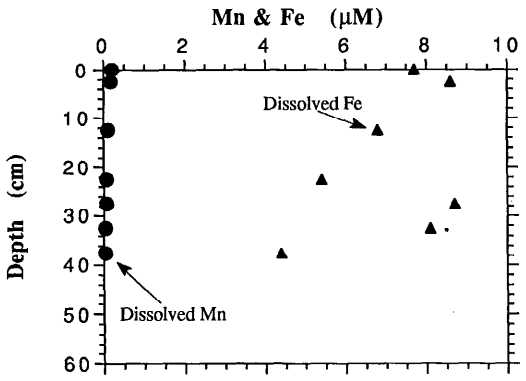

Fig. 3. Dissolved Fe and Mn in the pore waters of our Mangrove Lake core.

cept pH, display only a small variation in the top 15 cm, followed by substantial changes in the next 40 cm. The changes in total CO_2 and sulfate are many times larger than could be attributed to the salinity gradient. The dramatic increases in ΣH_2S, ΣNH_4, and reactive ΣPO_4 are all indicative of extensive sulfate reduction (*see* Orem et al. 1986). As we discuss later, calcium also decreases with depth more than can be explained by the salinity change. pH falls precipitously in the upper 15 cm, but exhibits only minor variability below this depth.

There is a paucity of solid Fe minerals in Mangrove Lake sediments as shown by our Fe analyses in Table 1. The solid Fe content is much lower than the average for normal marine sediments (e.g. Riley and Chester 1971). The dissolved Fe concentrations in the pore waters are also low (Fig. 3), and reflect the lack of an Fe source indicated by our solid phase analysis. The pore-water Mn concentrations are also shown in Fig. 3. Like Fe, Mn concentrations are low and probably reflect lack of source minerals. Overall, neither dissolved profile displays a consistent trend significant beyond the noise in the data.

Figure 4 displays the total ^{210}Pb in the solid fraction of this same core. The amount of supported ^{210}Pb could not be determined accurately for technical reasons. We believe, however, that there is very little supported ^{210}Pb in these sediments and that this profile is essentially equivalent to the excess ^{210}Pb in slope, if not in absolute value.

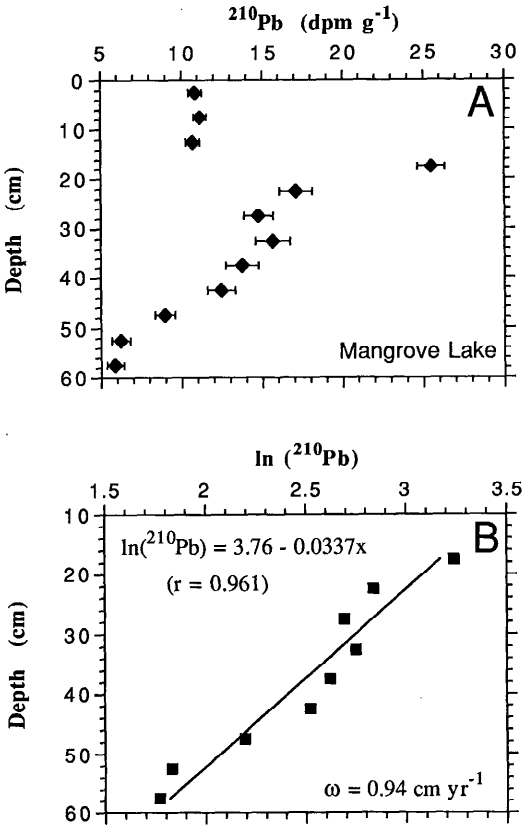

Fig. 4. ^{210}Pb profile in the solid fraction of sediment collected in Mangrove Lake. A. The raw data. B. Semi-logarithmic plot of the data below 15 cm (base of the mixed layer). The calculated burial rate is 0.94 cm yr^{-1}.

Our ^{210}Pb profile is characterized by three features, two of which might be expected, but the third is unusual. The top three data points are virtually identical and provide further evidence for a mixed zone of sediment in the top 15 cm. The vertical pore-water profiles in this upper zone also support the idea of a mixed zone. Below 15 cm, there is a nearly regular decrease in ^{210}Pb activity which suggests a regular burial-decay profile. What is not expected is the discontinuity at 15 cm, which is discussed later.

A standard ln(^{210}Pb) vs. depth plot for those data below 15 cm is shown in Fig. 4B. Interpreted as a burial-decay profile, this plot implies an accumulation rate, ω, of 0.94 cm yr^{-1} (or ~0.063 g cm^{-2} yr^{-1}). Orem et al. (1986) quoted a rate of 0.3 cm yr^{-1}, which

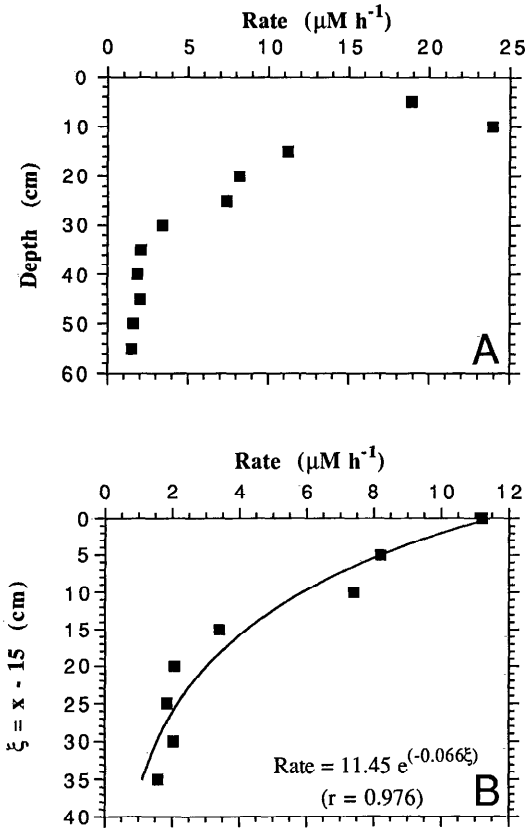

Fig. 5. Measured rates of sulfate reduction as a function of depth in a core from Mangrove Lake. A. Raw data. B. The best nonlinear fit to the data below the mixed layer. The implied rate constant for organic matter decay by sulfate reduction is 0.062 yr^{-1}.

probably is the historical average after compaction.

The measured rates of sulfate reduction are illustrated in Fig. 5A. There is an apparent maximum at 12 cm with a steady decline in rate thereafter. A nonlinear fit of an exponential to the data below 15 cm (Berner 1980) produces an exponential decay parameter, α, of 0.066 cm^{-1} ($r = 0.976$, where r is the absolute value of the correlation coefficient) (Fig. 5B). If there is indeed no appreciable mixing in the sediments below 15 cm, then $\alpha = k/\omega$, where k is the rate constant for decay. Substitution of our values of α and ω generates $k = 6.2 \times 10^{-2}$ yr^{-1}. This rate constant implies a half-life of ~11 yr for degradable organic matter in this lower depth interval.

Discussion and modeling

Sediment mixing—Before addressing the chemistry of this sediment, it is worthwhile discussing the mixing suggested by the ^{210}Pb and the pore-water profiles (e.g. salinity in Fig. 2). Bioturbating and irrigating organisms have not been reported in Mangrove Lake, and we observed none during our sampling. Consequently, we attribute the homogenized surface zone entirely to mixing by wind-induced waves or turbulence. We note however that the pore-water profiles measured by Mackenzie et al. (in press) from an earlier year do not appear to exhibit the degree of mixing suggested by our data. The intensity and depth of mixing may vary with time and location.

The penetration of the mixing is probably limited in part by the physical changes observed in the consistency of the sediment. Although porosity does not drop appreciably over the 50-cm sampling interval, the sediment does become observably less soupy, to the point where the deeper sediment appears more like a regular terrigenous sediment, except for its color (which is pine green). These changes cannot be related to compaction, but are due perhaps to the development of bonding between the organic matter particles. Hatcher et al. (1982) reported the presence of "gels" deeper in the sediment, and that may be the end result of the bonding process.

It is also interesting that the bottom of the mixed zone correlates with the apparent discontinuity in the ^{210}Pb profile. The connection, if any, is not obvious; we have strained to account for this phenomenon. A drop in the supply of ^{210}Pb relative to the input of organic matter is possible, or maybe it is due to some unexplained Pb chemistry. Transient remobilization and removal of ^{210}Pb could account for this profile. However, Benoit and Hemond (1990) associated such remobilization to the development of anoxic conditions. Based on the high organic matter content and its reactivity, we have no reason to believe that the sediment was not always anoxic. The cause of this peculiar ^{210}Pb profile remains obscure.

Pore-water chemistry—The pore waters of Mangrove Lake exhibit all the charac-

teristics of anoxic decomposition of organic matter (Hatcher 1978; Hatcher et al. 1982; Spiker and Hatcher 1984; Orem et al. 1986). What is interesting about this sapropel and its pore waters is that the diagenetic signals from the decay reaction are not encumbered or screened by competing or conflicting reactions. Our data present an unambiguous picture of anoxic decomposition in this sediment. Consequently, it is possible to make some quite definitive statements about the stoichiometry of the organic matter oxidation reaction and the depth relations between the various dissolved species that participate in this reaction. These topics are addressed below.

Stoichiometric relations—Stoichiometric modeling can be used not only to establish the C:N:P ratio of the decomposing organic matter (Berner 1977), but also to determine the amount of oxidant needed to oxidize a mole of organic matter and to ascertain if the products of this reaction, for example H_2S, participate in other reactions such as FeS formation. Such modeling can be done assuming the pore waters act as either a closed or an open system. Mackenzie et al. (in press) adopt the former approach, but we believe that an open system is the appropriate choice for the Mangrove Lake sediments.

To support this choice, we note that in a closed system, the transport of dissolved pore-water species must be dominated by advection due to burial. This situation is characterized by a large value of the Peclet number, Pe, which is defined as (at constant porosity)

$$\mathrm{Pe} = \frac{vL}{D_s} \qquad (1)$$

where v is the advective velocity of the pore water, L the depth scale of interest in the sediment (in our case 50 cm), and D_s a typical solute diffusion coefficient corrected for tortuosity.

There appears to be no externally impressed flow in the sediments of the lake. This statement is based on the results of the hydrologic survey conducted by Thomas et al. (1991) and the shape of our salinity profile. Therefore, we equate v to the burial velocity, ω. Free-solution diffusion coefficients of all the species of interest at 30°C and $S = 33$ are given in Table 2. An average value is ~ 500 cm^2 yr^{-1}. Furthermore, we can assume that for such a fine-grained sediment, the tortuosity, θ, can be related to porosity, φ, via the expression $\theta = \varphi^{-1}$ (Ullman and Aller 1982). The calculated value of Pe is then close to 0.1 and indicates that diffusion is 10 times more important than advection in this system. This Peclet number means that Mangrove Lake sediments do not act as a closed system with respect to diffusion, at least not on a 50-cm scale. We present below a mass balance argument that lends additional support to this statement.

Table 2. Molecular diffusion coefficients, D_i, for various species at $T = 30$°C and $S = 33$, in units of cm^2 yr^{-1}. Sources for these values are the same as those of Boudreau and Canfield (in press).

Species	D_i
CO_2	635
HCO_3^-	400
CO_3^{2-}	311
NH_3	749
NH_4^+	642
H_2S	647
HS^-	552
H_3PO_4	293
$H_2PO_4^-$	276
HPO_4^{2-}	248
PO_4^{3-}	206
SO_4^{2-}	348
OH^-	1,710
H^+	2,957
Ca^{2+}	258

Berner (1977) has presented the theory of stoichiometric modeling for open systems. This model makes use of the steady state assumption. Although we have already discussed temporal changes in salinity due to excess evaporation, we note that the concentration changes resulting from the salinity gradient are relatively modest (<10% in the zone below 15 cm). The observed changes in sulfate, sulfide, carbonate alkalinity, and nutrients are far larger than can be attributed to this effect. Thus, we advance that the profiles reflect essentially steady state organic matter decay by sulfate reduction, onto which is imposed a small

transient. The results given below suggest that this transient is buried within the noise in the data.

The ratio of the change in the concentrations of two species involved in sulfate reduction in an open system is given by (Berner 1977, 1980)

$$\frac{\partial C_n}{\partial C_m} = \frac{\gamma_n}{\gamma_m}\left[\frac{D_m k(\omega\theta)^{-2} + (1 + K_m)}{D_n k(\omega\theta)^{-2} + (1 + K_n)}\right] \quad (2)$$

where C_m and C_n are the concentrations of the mth and nth species, D_m and D_n the molecular diffusivities of these species, θ the tortuosity, K_m and K_n the respective adsorption constants, and γ_n and γ_m the stoichiometric coefficients of these species in the sulfate reduction reaction

$$(CH_2O)_x(NH_3)_y(H_3PO_4)_z + x/2SO_4^{2-} \rightarrow xHCO_3^- + x/2H_2S + yNH_3 + zH_3PO_4. \quad (3)$$

The constant k is the rate constant for reaction 3 as determined from a plot like Fig. 5, and x, y, and z are the actual stoichiometric coefficients for C, N, and P in reaction 3, traditionally taken as $x = 106$, $y = 16$, and $z = 1$.

We begin our data analysis by considering the relationship between SO_4^{2-} and ΣH_2S. If H_2S and HS^- are not involved in the precipitation of FeS or the formation of organic S compounds, there should be a simple linear relationship predictable via Eq. 2. This calculation can be simplified further by noting that adsorption is usually considered negligible for sulfate and sulfide ($K_{SO_4} = K_{\Sigma H_2S} = 0$). Additionally, $D_s k/\omega^2 \gg 1$ for both species; thus, Eq. 2 reduces to

$$\left(\frac{\partial \Sigma H_2S}{\partial SO_4}\right)_{theor.} = -\frac{D_{SO_4}}{D_{\Sigma H_2S}} \quad (4)$$

where $D_{\Sigma H_2S}$ is the "mean" molecular diffusion coefficient of the H_2S-HS^- pair, and D_{SO_4} is the molecular diffusion coefficient of SO_4^{2-} (Table 2). The calculated relative abundances of H_2S and HS^- are 30 and 70%. The mean diffusion coefficient, $D_{\Sigma H_2S}$, is then weighted in this proportion to arrive at 579.5 $cm^2\ yr^{-1}$. Therefore, the predicted ratio is

$$\left(\frac{\partial \Sigma H_2S}{\partial SO_4}\right)_{theor.} = -0.601. \quad (5)$$

The actual ratio can be calculated as the slope of a plot of SO_4^{2-} vs. ΣH_2S (Fig. 6A),

$$\left(\frac{\partial \Sigma H_2S}{\partial SO_4}\right)_{obs.} = -0.566. \quad (6)$$

The 6% difference between observed and theoretical ratios is close to the analytical errors (i.e. ~5% for ΣH_2S and 1% for SO_4^{2-}) and is consistent with little or no sulfide precipitation. This finding is explained by the low availability of Fe in these sediments (Table 1) which prevents FeS formation. The formation of organic S compounds also seems to be negligible, as there is no systematic increase in S content with depth (Table 1).

The standard stoichiometry of reaction 3 requires the production of 2 units of ΣCO_2 for the consumption of 1 unit of SO_4^{2-} and the appearance of 1 unit of ΣH_2S. [We deal with ΣCO_2 rather than the more obvious carbonate alkalinity because a small, but appreciable, portion of the HCO_3^- generated by reaction 3 has converted to CO_2(aq) at the in situ pH values.] On the basis of the same logic used to derive Eq. 4, this leads to the theoretical ratios

$$\left(\frac{\partial \Sigma CO_2}{\partial \Sigma H_2S}\right)_{theor.} = \frac{2D_{\Sigma H_2S}}{D_{\Sigma CO_2}} \quad (7)$$

and

$$\left(\frac{\partial \Sigma CO_2}{\partial SO_4}\right)_{theor.} = \frac{2D_{SO_4}}{D_{\Sigma CO_2}}. \quad (8)$$

The ΣCO_2 is ~90% HCO_3^- and 10% CO_2 (aq); consequently, we set $D_{\Sigma CO_2} = 423$ $cm^2\ yr^{-1}$ based on the values in Table 2. The theoretical values of the ratios are

$$\left(\frac{\partial \Sigma CO_2}{\partial \Sigma H_2S}\right)_{theor.} = 2.71 \quad (9)$$

and

$$\left(\frac{\partial \Sigma CO_2}{\partial SO_4}\right)_{theor.} = -1.64. \quad (10)$$

The actual fits to the data (Fig. 6B and D) give

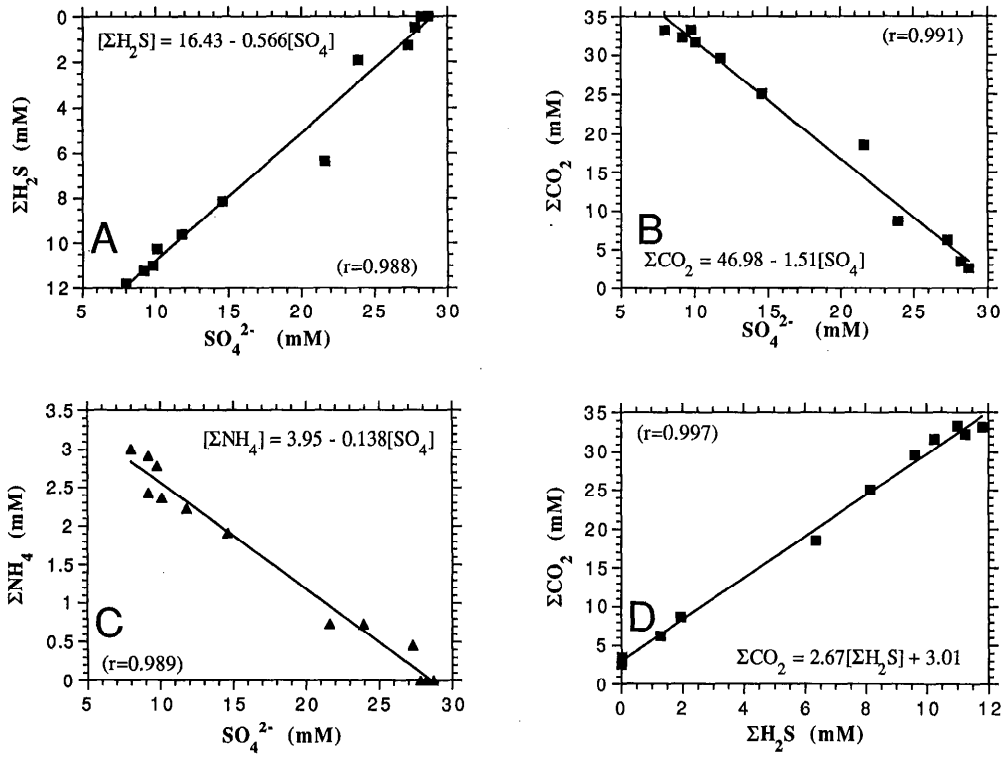

Fig. 6. Stoichiometric plots for the primary species involved in reaction 3 and the linear best-fits to these data. Each diagram also contains the equation describing this linear fit and its (absolute) correlation coefficient, *r*.

$$\left(\frac{\partial \Sigma CO_2}{\partial \Sigma H_2S}\right)_{obs.} = 2.67 \qquad (11)$$

and

$$\left(\frac{\partial \Sigma CO_2}{\partial SO_4}\right)_{obs.} = -1.51. \qquad (12)$$

The two observed ratios are within 1.5 and 8% of the theoretical values if the traditional stoichiometry of reaction 3 is correct. Any disagreement between observed and theoretical values is well within the analytical errors in the data and the possible cumulative ~5% error in the calculated conversion of titration alkalinity to A_c and ΣCO_2. There seems to be no reason to invoke nonstandard organic C : SO_4 stoichiometry.

All the above assumes constant molecular diffusion coefficients, and we know there is mixing in the upper 15 cm. The plots in Fig. 6 include data from the mixed zone; consequently, the observed ratios should not be constants in the presence of this mixing. Specifically, the theoretical ratio in the presence of mixing should read

$$\left(\frac{\partial \Sigma H_2S}{\partial SO_4}\right)_{theor.} = -\frac{(D_{mix} + D_{SO_4}\theta^{-2})}{(D_{mix} + D_{H_2S-HS}\theta^{-2})} \qquad (13)$$

where D_{mix} is the depth-dependent component of the effective diffusivity due to physical mixing. We expect D_{mix} to be the same for all species. If $D_{mix} \gg D_{SO_4}$ and $D_{\Sigma H_2S}$ in the mixed zone, then

$$\left(\frac{\partial \Sigma H_2S}{\partial SO_4}\right)_{theor.} = -1, \qquad (14)$$

and as D_{mix} decreases with depth, this ratio goes to 0.601 as given by Eq. 5. On a ΣH_2S

vs. SO_4 plot, the slope should change with depth, which does not occur within the resolution of the plots in Fig. 6 because the mixed-zone data points bunch together near the SO_4^{2-} axis. Mixing is so efficient that gradients are obliterated in this zone. All the trends in this figure are defined by points below the mixed zone where molecular diffusion is the dominant transport process.

A primary application of stoichiometric modeling is determination of the C:N:P ratio of the decomposing organic matter. Theoretical stoichiometric modeling for total dissolved ammonium, ΣNH_4, would suggest

$$\frac{y}{x} = -\frac{\left[\frac{D_{\Sigma NH_4}k}{(\omega\theta)^2} + (1 + K_{NH_4})\right]}{2\left[\frac{D_{SO_4}k}{(\omega\theta)^2} + 1\right]}\left(\frac{\partial \Sigma NH_4}{\partial SO_4}\right)_{obs.} \quad (15)$$

where K_{NH_4} is the adsorption coefficient for ΣNH_4 and the stoichiometric constants x and y are defined following Eq. 3. The ratio $\partial\Sigma NH_4 : \partial SO_4$ is obtained from the linear regression shown in Fig. 6C.

We do not have any measurements of K_{NH_4}; regardless, we can place reasonable limits on this parameter and, consequently, on the C:N ratio. As a lower bound, K_{NH_4} can be set to zero. To establish an upper bound, we note that Rosenfeld (1979) measured K_{NH_4} in various types of marine sediments. He found that it increased with the amount of organic matter in the sediment. His most organic-rich sediment contained 15% organic matter and had $K_{NH_4} = 0.8$. If K_{NH_4} scales linearly with organic matter content, then the K_{NH_4} for Mangrove Lake should be ~5, which we advance as our upper bound.

With these lower and upper bounds on K_{NH_4}, Eq. 15 generates y/x values of 0.259 and 0.145. These values correspond to C:N ratios of 3.86–6.87. For comparison, the Redfield C:N ratio is 6.67, and the measured C:N ratio in the solids varies from 8.7 to 16.5 (Table 1; Hatcher et al. 1982; Orem et al. 1986). Therefore, the decay process regenerates nitrogen preferentially to carbon compared to the relative abundance of these elements in the solid organic matter (Rosenfeld 1981). Although the C:N of the solids is not particularly different than that measured in other shallow-water marine sediments, i.e. 9.0–13.5 (Nissenbaum et al. 1972; Krom and Berner 1981; Klump and Martens 1987), the regeneration ratio is at the low-end of the range reported in the marine literature (e.g. 8.8–9.9 at the FOAM site, Berner 1977; Krom and Berner 1981; 11.0 in a Swedish coastal sediment, Anderson et al. 1986; 4.5–9.15 at Cape Lookout Bight, Klump and Martens 1987).

This modeling technique cannot be used to determine a C:P ratio. As seen in Fig. 2 the reactive-P profile exhibits a subsurface maximum, which probably reflects absorption onto $CaCO_3$ surfaces, but possibly also the precipitation of a phosphate mineral or perhaps sequestering of P into an organic-P pool. A plot of SO_4^{2-} vs. ΣPO_4 (not shown) suggests a highly curved relationship consistent with removal of reactive P.

Depth relations—Stoichiometric modeling tells only how the accumulation of a pore-water species compares to another. Questions relating to chemical fluxes and the "openness" of the sediment to exchange require modeling the depth profiles for the species of interest.

To begin, the steady state constant-porosity diagenetic equation for dissolved sulfate is

$$D_{SO_4}\frac{d^2[SO_4]}{d\xi^2} - R\exp(-\alpha\xi) = 0; \quad (16)$$

it applies only below the mixed zone ($\xi = x - 15$ cm) and where we have dropped the advective term because $Pe \ll 1$. As stated above, we will verify the validity of this assumption and the open nature of this sediment with a flux balance. The constant α is the attenuation of the sulfate reduction reaction with depth (*see Fig. 5*), and R is the magnitude of the rate of this reaction at $\xi = 0$.

The well-known solution to Eq.16 is

$$[SO_4] = A + B\xi + C\exp(-\alpha\xi) \quad (17)$$

where A and B are integration constants, and

$$C \equiv R\theta^2(D_{SO_4}\alpha^2)^{-1}. \quad (18)$$

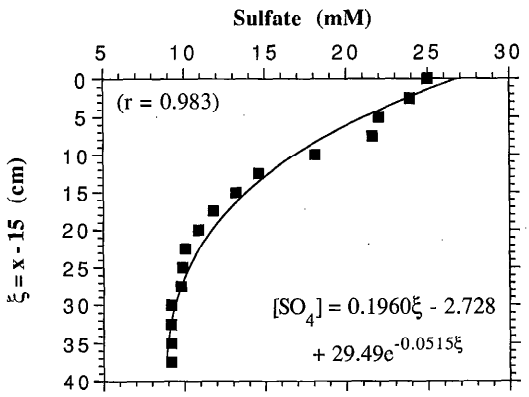

Fig. 7. Sulfate data from below the mixed zone and the best nonlinear four-parameter fit to the data (i.e. parameters *A, B, C,* and α in Eq. 17). Also shown is the resulting equation for this fit and its (absolute) correlation coefficient, *r*.

Normally, *A* and *B* are determined from boundary conditions, where the SO_4^{2-} concentrations at $\xi = 0$ and $\xi = 40$ cm are treated as known values and substituted into Eq. 17. There is no reason to believe, however, that these values are better known than the sulfate concentrations at any other depth; so, a nonlinear fit of Eq. 17 is applied to all points in the profile to define *A* and *B*.

With this procedure it is also possible to arrive at a better appreciation for the validity of using the experimental value of α calculated in Fig. 5. To this end, we can perform a fit with α as an unknown parameter and another with the value from Fig. 5, comparing the goodness-of-fit in each case. A four-parameter (i.e. *A, B, C,* and α) fit to the SO_4^{2-} data is shown in Fig. 7. The calculated α value is 0.0515 cm^{-1} with $r = 0.983$. Figure 8A illustrates a three-parameter fit (*A, B,* and *C*), but with $\alpha = 0.066$ cm^{-1} as in Fig. 5 ($r = 0.982$). The two values of α differ by $\leq 22\%$, and the difference in their corresponding *r* values is not significant. Thus, the value of α found in Fig. 5 provides a good description of the dissolved sulfate data. The experimental value of α should also generate good fits to the other porewater profiles, which is verified in Fig. 8B, C. The predictions for the total dissolved NH_4 profile are shown in Fig. 9 for the two limiting K_{NH_4} values. Again the predicted profile based on the α from Fig. 5 and the

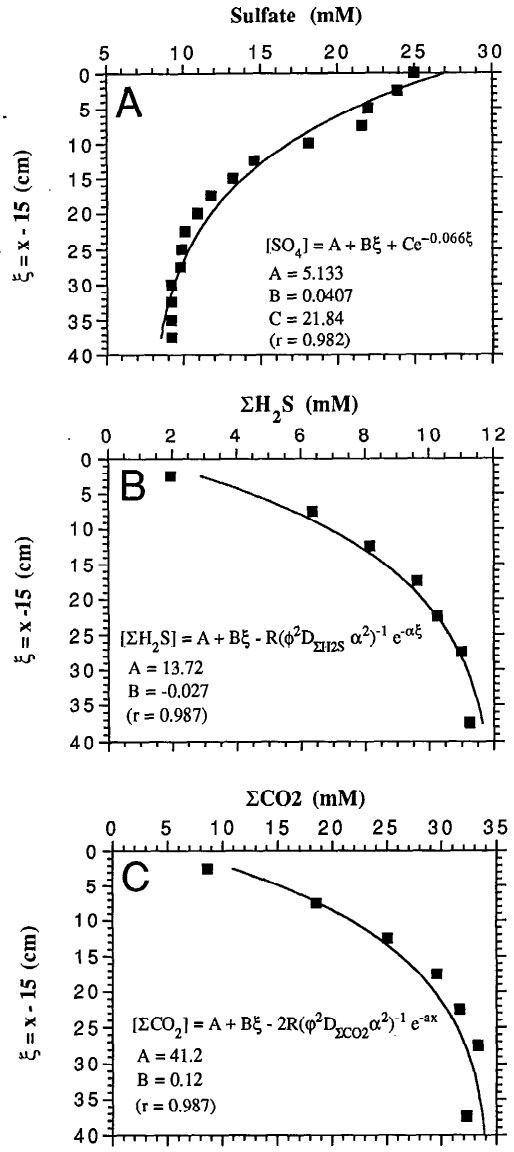

Fig. 8. A. The best three-parameter fit to the SO_4^{2-} profile with the experimentally determined α value (Fig. 5) for sulfate reduction (i.e. parameters A, B, and C in Eq. 17). B, C. Profiles for ΣH_2S and CO_2, based on the fit to the SO_4^{2-} profile in the top diagram. (The goodness-of-fit in each case is given by the *r*-correlation coefficient.)

R value from the SO_4^{2-} profile provides a good fit to the data.

We are now in a position to make quantitative estimates of the diffusive and advective fluxes at the top of the unmixed zone

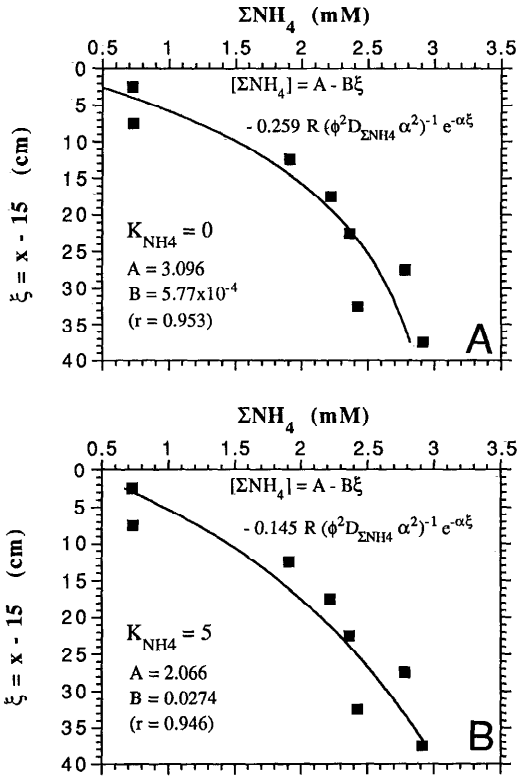

Fig. 9. Predicted fits to the total NH_4^+ profiles, based on the fit to the SO_4^{2-} profile in Fig. 8. A. The result with no ΣNH_4 adsorption, $K_{NH_4} = 0$, represents the lower bound on possible K_{NH_4} values. B. The result with $K_{NH_4} = 5$, represents the upper bound on possible K_{NH_4} values.

($\xi = 0$ or $x = 15$ cm) and to formulate a mass balance that provides an alternative method for determining the degree of openness of this system. The diffusive flux at the base of the mixed zone, F_D, is given by Fick's first law modified for the presence of the fine-grained solids (Berner 1980; Ullman and Aller 1982)

$$F_D = -\varphi^3 D_{SO_4} \left.\frac{d[SO_4]}{d\xi}\right|_{\xi=0}. \quad (19)$$

With the fit found in Fig. 7,

$$\left.\frac{d[SO_4]}{d\xi}\right|_{\xi=0} = B - 0.066C, \quad (20)$$

which leads to our estimate of the diffusive flux of sulfate into the unmixed zone $F_D = 425$ μmol cm^{-2} yr^{-1}.

To compare, the advective flux is given by

$$F_A = \varphi\omega[SO_4]_{\xi=0}, \quad (21)$$

from which we estimate a value of $F_A = 22.5$ μmol cm^{-2} yr^{-1}. Therefore, the advective flux is only 5% of the diffusive flux into the unmixed zone. This readily confirms our prediction of an open system based on calculation of the Peclet number.

It is also important to verify whether the calculated fluxes of sulfide and ΣCO_2 are consistent with the sulfate flux. The flux of sulfide calculated from the nonlinear fit is -423 μmol cm^{-2} yr^{-1}, within 0.5% of the expected value based on the sulfate flux. The ΣCO_2 flux is -815 μmol cm^{-2} yr^{-1}, which is lower than expected by ~4%. This small discrepancy could be due to the uncertainties in converting titration alkalinity to carbonate alkalinity (which potentially could amount to an error of as much as 5%) or the small amount of $CaCO_3$ precipitation. Regardless, these mass balances illustrate the consistency of our calculations.

As a final check on our stoichiometric modeling of the previous section, we can use the results of the diagenetic model to show that only a small fraction of the sulfide produced by sulfate reduction reacts and is buried with the solid phase. The total amount of sulfide produced in the 40-cm reaction zone, $\bar{R}$, is given by

$$\bar{R} = R \int_0^{40} \exp(-\alpha\xi)\, d\xi \quad (22)$$

where R is calculated from the curve-fit parameter, C, and Eq. (19). The result is $\bar{R} \approx 440$ μmol S cm^{-2} yr^{-1}. The burial flux of total S is only 30 μmol cm^{-2} yr^{-1}. Therefore, little of the sulfide is reacting with either Fe or organic matter to be buried; most must be diffusing out the top of the sediment column.

Carbonate chemistry—Figure 10 displays the ion concentration product (ICP) of Ca^{2+} and CO_3^{2-} and the stoichiometric K^*_{sp} for calcite and aragonite as calculated from the formulas of Mucci (1983) and UNESCO (1987). The error bars represent a 5% possible uncertainty in the ICP values. This plot indicates that the overlying waters are

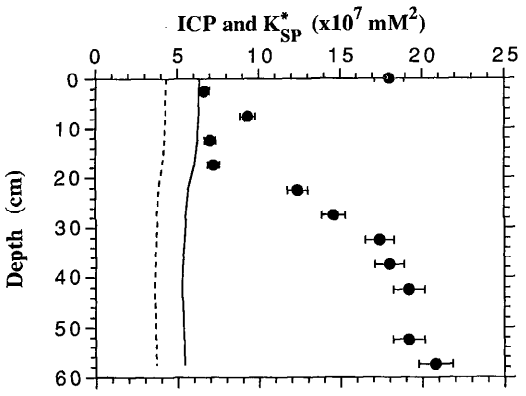

Fig. 10. The ion concentration product (ICP) of Ca^{2+} and CO_3^{2-} and the K^*_{sp} for aragonite and calcite in pore waters of Mangrove Lake. ICP > K^*_{sp} indicates supersaturated conditions, and ICP < K^*_{sp} characterizes undersaturated pore waters. Dashed line—K^*_{sp} (calcite); solid line—K^*_{sp} (aragonite). Error bars represent a 5% possible uncertainty in ICP values.

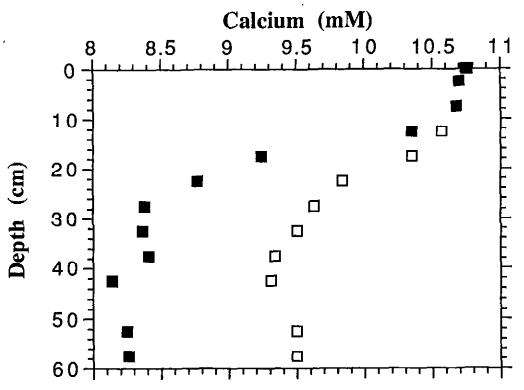

Fig. 11. The actual dissolved Ca profile in pore waters of Mangrove Lake (■) and the theoretical profile (□) assuming conservative behavior with salinity.

supersaturated with respect to both minerals, but that ICP values near equilibrium with aragonite are rapidly established in the mixed layer. Below the mixed zone, the increasing carbonate alkalinity coupled with a constant pH produces increasing levels of supersaturation with depth.

The drop in ICP is due to two contributing processes. The first is a decrease in the CO_3^{2-} concentration that accompanies the large drop in pH in the upper portion of the sediments. This drop in pH accompanies both oxic organic matter decay and the oxidation of reduced by-products of sulfate reduction (Boudreau and Canfield in press). The upward transport of alkalinity is insufficient to overcome this effect.

The second process appears to be carbonate-mineral precipitation. Evidence for active $CaCO_3$ precipitation in the upper 20 cm of this sapropel comes from the Ca profile. If we calculate the Ca profile based on conservative behavior with salinity, then we obtain the empty squares plotted in Fig. 11. The actual data are given by the filled squares and are displaced to appreciably lower Ca concentrations. The deficiency between observed and conservative profiles is due to removal of Ca, which we believe is due to $CaCO_3$ formation. The steeper Ca gradient in the mixed zone implies further that this precipitation occurs mostly in this zone, as suggested by the ICP vs. K^*_{sp} plot. The difference between the actual and observed Ca concentrations is essentially constant below 17.5 cm which also indicates that the precipitation is in the mixed zone. In addition, the stoichiometric model results argue strongly that there is virtually no carbonate removal below 15 cm.

We have not been able, however, to identify any carbonate mineral(s) in the solid phase that could account for the observed saturationlike values in the mixed zone. The only carbonates we and others (Hatcher et al. 1982) have located in this sapropel are small scattered ostracods (*Cyprideis* sp.) that are composed of a pure to low Mg (<6.5%) calcite as determined by X-ray diffraction analysis. This material should not produce the observed solubility trend.

Conclusions

We have collected a suite of geochemical profiles in both the pore waters and solids that define the early diagenesis of organic matter in the sapropel of Mangrove Lake. Diagenetic modeling of these data reveals that molecular diffusion dominates transport of pore-water species in the first 40 cm below the surficial mixed zone. This finding has been verified by calculating the Peclet number and comparing the calculated diffusive and advective fluxes of dissolved sulfate, sulfide, and carbonate. Consequently, this pore-water system should not be con-

sidered "closed." In fact, the diagenesis of this sapropel follows almost perfectly the path predicted by open-system stoichiometric theory (Berner 1977, 1980), with dissolved reactive P as the only obvious exception. The adherence of the dissolved sulfide system to our stoichiometric model is attributable to the lack of Fe-sulfide precipitation, due to limited Fe availability, and minor incorporation into S-bearing organic compounds. Similarly, Mn minerals do not appear to play an important role in the diagenesis of this sediment. In addition, we have determined that the pore waters are nearly saturated with respect to aragonite in the surficial mixed zone, but supersaturated in the sediments below. Comparison of the measured Ca profile with that expected for conservative behavior indicates that active precipitation of a carbonate mineral is restricted to the mixed zone. Overall, the basic diagenesis of the Mangrove Lake sapropel is quite intelligible from a theoretical point of view; such an environment is quite valuable for the study of more complex diagenetic processes, such as the control of pore-water pH.

References

ALLER, R. C. 1980. Diagenetic processes near the sediment–water interface of Long Island Sound. 1. Decomposition and nutrient element geochemistry (S, N, P). Adv. Geophys. **22:** 237–350.

ANDERSON, L. G., AND OTHERS. 1986. Benthic respiration measured by total carbonate production. Limnol. Oceanogr. **31:** 319–329.

BATES, R. G. 1973. Determination of pH: Theory and practice. Wiley-Interscience.

BENOIT, G., AND H. F. HEMOND. 1990. ^{210}Po and ^{210}Pb remobilization from lake sediments in relation to iron and manganese cycling. Environ. Sci. Technol. **24:** 1224–1234.

BERNER, R. A. 1977. Stoichiometric models for nutrient regeneration in anoxic sediments. Limnol. Oceanogr. **22:** 781–786.

———. 1980. Early diagenesis: A mathematical approach. Princeton.

BOUDREAU, B. P., AND D. E. CANFIELD. 1988. A provisional diagenetic model for pH in anoxic porewaters: Application to the FOAM site. J. Mar. Res. **46:** 429–455.

———, AND ———. In press. A comparison of closed and open system models for porewater pH and calcite-saturation state. Geochim. Cosmochim. Acta.

CANFIELD, D. E. 1989. Reactive iron in marine sediments. Geochim. Cosmochim. Acta **53:** 619–632.

———, AND R. RAISWELL. 1991. Carbonate preservation in Modern sediments, p. 337–387. *In* P. A. Allison and D. G. Briggs [eds.], Taphonomy: Releasing the information locked in the fossil record. Plenum.

———, ———, J. T. WESTRICH, C. M. REAVES, AND R. A. BERNER. 1986. The use of chromium reduction in the analysis of reduced sulfur in sediments and shales. Chem. Geol. **54:** 149–155.

CLINE, J. 1969. Spectrophotometric determination of hydrogen sulfide in natural waters. Limnol. Oceanogr. **14:** 454–458.

EMERSON, S. R., AND OTHERS. 1980. Early diagenesis in sediments from the eastern equatorial Pacific. 1. Pore water nutrient and carbonate results. Earth Planet. Sci. Lett. **49:** 57–80.

FROELICH, P. N., AND OTHERS. 1979. Early oxidation of organic matter in pelagic sediments of the eastern equatorial Atlantic: Suboxic diagenesis. Geochim Cosmochim. Acta **43:** 1075–1090.

GRAN, G. 1952. Determination of the equivalence point in potentiometric titrations. Part 2. Analyst **77:** 661–671.

GRASSHOFF, K. 1976. Methods of seawater analysis. Verlag Chemie.

HANSSON, I. 1973. A new set of pH-scales and standard buffer for sea water. Deep-Sea Res. **20:** 479–491.

HATCHER, P. G. 1974. A study of the organic geochemistry of Mangrove Lake, Bermuda. M.S. thesis, Univ. Miami. 231 p.

———. 1978. The organic geochemistry of Mangrove Lake, Bermuda. NOAA Prof. Pap. 10. 92 p.

———, AND OTHERS. 1982. Organic geochemistry and pore water chemistry of sediments from Mangrove Lake, Bermuda. Org. Geochem. **4:** 93–112.

JAHNKE, R. A., D. HEGGIE, S. EMERSON, AND V. GRUNDMANIS. 1982. Pore waters of the central Pacific Ocean: Nutrient results. Earth Planet. Sci. Lett. **61:** 233–256.

JOHANSSON, O., AND M. WEDBORG. 1979. Stability constants of phosphoric acid in seawater of 5–40‰ salinity and temperatures of 5–25°C. Mar. Chem. **8:** 57–69.

———, AND ———. 1980. The ammonia-ammonium equilibrium in seawater at temperatures between 5 and 25°C. J. Solut. Chem. **9:** 37–44.

JØRGENSEN, B. B. 1978. A comparison of methods for the quantification of bacterial sulfate reduction in coastal sediments. 1. Measurement with radiotracer techniques. Geomicrobiol. J. **1:** 11–27.

KLUMP, J. V., AND C. S. MARTENS. 1987. Biogeochemical cycling in an organic-rich marine basin. 5. Sedimentary nitrogen and phosphorus budgets based upon kinetic models, mass balances, and the stoichiometry of nutrient regeneration. Geochim. Cosmochim. Acta **51:** 1161–1173.

KROM, M. D., AND R. A. BERNER. 1981. The diagenesis of phosphorus in a nearshore marine sediment. Geochim. Cosmochim. Acta **45:** 207–216.

LEBEL, J., AND A. POISSON. 1976. Potentiometric determination of calcium and magnesium in seawater. Mar. Chem. **4:** 321–332.

MACKENZIE, F. T., S. VINK, R. WOLLAST, AND L. CHOU. In press. Comparative geochemistry of marine

saline lakes. *In* A. Lerman [ed.], Lakes. V. 2. Springer.

MACKIN, J. E., AND R. C. ALLER. 1989. The nearshore marine estuarine chemistry of dissolved aluminum and rapid authigenic mineral precipitation. Aquat. Sci. **1:** 537–554.

MILLERO, F. J. 1979. The thermodynamics of the carbonate system in seawater. Geochim. Cosmochim. Acta **43:** 1651–1661.

———, T. PLESE, AND M. FERNANDEZ. 1988. The dissociation of hydrogen sulfide in seawater. Limnol. Oceanogr. **33:** 269–274.

MUCCI, A. 1983. The solubility of calcite and aragonite in seawater at various salinities, temperatures, and one atmosphere total pressure. Am. J. Sci. **283:** 789–799.

———. 1991. A potentiometric back-titration method for the determination of sulfate in seawater and marine pore waters. Limnol. Oceanogr. **36:** 409–412.

NISSENBAUM, A., B. J. PRESLEY, AND I. R. KAPLAN. 1972. Early diagenesis in a reducing fjord, Saanich Inlet, British Columbia. 1. Chemical and isotopic changes in major components of interstitial waters. Geochim. Cosmochim. Acta **32:** 1007–1027.

OREM, W. H., P. G. HATCHER, E. C. SPIKER, N. M. SZEVERENYI, AND G. E. MACIEL. 1986. Dissolved organic matter in anoxic waters from Mangrove Lake, Bermuda. Geochim. Cosmochim. Acta **50:** 609–618.

REEBURGH, W. S. 1967. An improved interstitial water sampler. Limnol. Oceanogr. **12:** 163–165.

RILEY, J. P., AND R. CHESTER. 1971. Introduction to marine chemistry. Academic.

ROSENFELD, J. K. 1979. Ammonium adsorption in nearshore anoxic sediments. Limnol. Oceanogr. **24:** 356–364.

———. 1981. Nitrogen diagenesis in Long Island Sound sediments. Am. J. Sci. **281:** 436–462.

SPIKER, E. C., AND P. G. HATCHER. 1984. Carbon isotope fractionation of sapropelic organic matter during early diagenesis. Org. Geochem. **4:** 283–290.

SMITH, J. N., AND A. WALTON. 1980. Sediment accumulation rates and geochronologies measured in the Saguenay Fjord using the Pb-210 dating method. Geochim. Cosmochim. Acta **44:** 225–240.

THODE-ANDERSEN, S., AND B. B. JØRGENSEN. 1989. Sulfate reduction and the formation of ^{35}S-labeled FeS, FeS_2 and S^0 in coastal marine sediments. Limnol. Oceanogr. **34:** 793–806.

THOMAS, M. L. H., K. E. EAKINS, AND A. LOGAN. 1991. Physical characteristics of the anchialine ponds of Bermuda. Bull. Mar. Sci. **48:** 125–136.

ULLMAN, W. J., AND R. C. ALLER. 1982. Diffusion coefficients in nearshore marine sediments. Limnol. Oceanogr. **27:** 552–556.

UNESCO. 1987. Thermodynamics of the carbon dioxide system in seawater. Tech. Pap. Mar. Sci. 51. 55 p.

Submitted: 11 June 1991
Accepted: 5 November 1991
Revised: 21 July 1992